IJRD International Journal of Research & Development Organisation

Journal Of Electrical And Electronics Engineering

Analysis of Over-Modulation Technique for SVPWM VFI on the Performance of Induction Motor Drive

HAFSA MUZAFAR
M.Tech. Power Electronics and Drives
Department of Electrical Engineering
Dehradun Institute of Technology University
Dehradun

Harsha Saroa
Assistant Professor
Department of Electrical Engineering
Dehradun Institute of Technology University
Dehradun

ABSTRACT:

This paper focuses on development of SVPWM that fully covers the over modulation region. The model of a three-phase voltage source inverter is discussed based on space vector theory. The conventional SVPWM technique has been deeply studied. All the study has been made in MATLAB /SIMULINK environment**.**

Keywords- Modulation Index, SVPWM, Overmodulation, Crossover angle, Holding angle.

1. INTRODUCTION:

In undermodulation region the peak fundamental voltage can be as high as $0.577V_{dc}$ (2-33) reference vector makes a circular trajectory. This value can be exceeded during overmodulation region when the desired trajectory partly passes outside of the hexagon. The modulation index of the overmodulation region ranges from 0.907 to1 [**2**]. Overmodulation region is divided into two regions with two modes of operation depending on the modulation index values.

Overmodulation region-1

Overmodulation region-2

1.1 Overmodulation region-1

The overmodulation region starts when the reference voltage exceeds the hexagon boundary, and the MI is larger than 0.907.The boundary between the undermodulation zone and overmodulation region 1 starts when MI=0.907and the boundary between the overmodulation region 1 and the overmodulation region 2 starts when MI=0.952. In overmodulation mode-1 as shown in Fig.2-9 V_{ref} crosses the hexagon at two points in each sector. There is loss of fundamental voltage in this region. To compensate this loss, that is to match reference voltage vector V_{ref} with average output voltage, a modified reference voltage trajectory that remains partly on hexagon and partly on circle is selected. The output voltage waveform is approximated by linear segments on the hexagon trajectory and by sinusoidal segments on the circular trajectory.

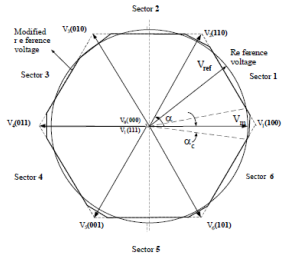

Fig. Space vectors of three-phase inverter showing reference voltage trajectory and segments of adjacent voltage vectors for overmodulation region 1

The circular part of modified trajectory has radius V_m which is greater than V_{ref} and crosses hexagon at angle α_c as shown in Fig.2-9. When V_m is in circular trajectory it follows (2-30)-(2-31) but with modified reference voltage.

During hexagon trajectory only the active vectors are taken into account thus time t_0 vanishes, giving only t_a and t_b time intervals which can be expressed a follows:

$$t_a = \frac{T_S}{2}\left[\frac{\sqrt{3}\cos\alpha - \sin\alpha}{\sqrt{3}\cos\alpha + \sin\alpha}\right]$$

$$t_b = \frac{T_S}{2} - t_a$$

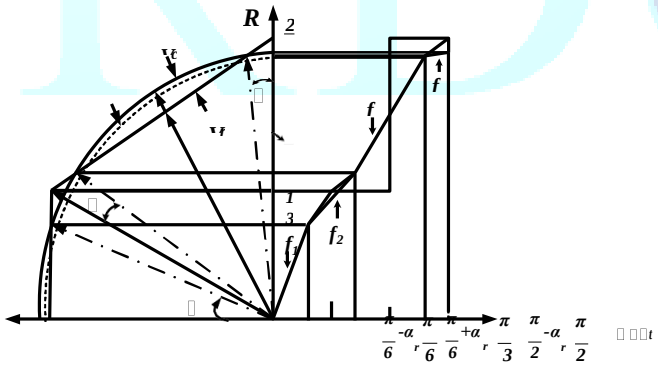

Fig. Trajectory of reference voltage vector and phase for overmodulation region 1

Fig.shows the trajectory of three voltage vectors rotating in a complex plane (left part) and the phase voltage waveform of an actual voltage reference vector (V^*_c) transformed in a time domain (right part),which is modulated actually by the inverter. Here, the crossover angle (α_c) denotes a reference angle measured from the vertex to the intersection of the compensated voltage vector trajectory with the side. In both side regions of each triangle sector to α_c, V_c^* is used to compensate the voltage loss due to the excess of the outer hexagon, generating the maximum voltage value to follow the outer hexagon between those two

regions.

For a given voltage reference, the phase voltage waveform is divided into four segments. The voltage equations in each segments is given by following equations .

$$f_1 = m_1 \times \theta, \qquad 0 \le \theta \le \left(\frac{\pi}{6} - \alpha_c\right)$$

$$f_2 = V_{mod1} \times \sin\theta, \qquad \left(\frac{\pi}{6} - \alpha_c\right) \le \theta \le \left(\frac{\pi}{6} + \alpha_c\right)$$

$$f_3 = A + \frac{m_1}{2} \times \theta, \qquad \left(\frac{\pi}{6} + \alpha_c\right) \le \theta \le \left(\frac{\pi}{2} - \alpha_c\right)$$

$$f_4 = V_{mod1} \times \sin\theta, \qquad \left(\frac{\pi}{2} - \alpha_c\right) \le \theta \le \frac{\pi}{2}$$

Where, $\theta = \omega t$, $m_1 = 2V_{dc}/\pi$=linear segment slope =1, $A = V_{dc}/6$ and V_m is reference voltage for region 1 and is defined as function of α_c by equating(2-39) and (2-40) for angle $\left(\frac{\pi}{2} - \alpha_c\right)$ as

$$V_{mod1} = \frac{V_{dc}(2 \times pi - 3 \times \alpha_c)}{3 \times pi \times \cos(\alpha_c)}$$

Hence, the peak value of the fundamental output voltage (V_{1_mod1}) can be found with the help of Fourier series expansion by (2-42) using (2-37)-(2-40) as:

$$V_{1\_mod1} = \frac{4}{\pi}\left[\begin{array}{ll} \int_0^{\pi/6-\alpha_r} f_1 \sin\theta d\theta + & \int_{\pi/6-\alpha_r}^{\pi/6+\alpha_r} f_2 \sin\theta d\theta \\ + \int_{\pi/6+\alpha_r}^{\pi/2-\alpha_r} f_3 \sin\theta d\theta + & \int_{\pi/2-\alpha_r}^{\pi/2} f_4 \sin\theta d\theta \end{array}\right]$$

Therefore

$$m\_01 = \frac{V_m}{\frac{2}{\pi}V_{dc}} = \frac{\pi V_m}{2V_{dc}} = \frac{1}{\pi}\left\{\begin{array}{l} \left(3\sqrt{3}\alpha_c + 3\right)\cos\alpha_c \\ + \left(3\alpha_c - 2\pi - 3\sqrt{3}\right)\sin\alpha_c + \dfrac{\left(2\pi\alpha_c - 3\alpha_c^2\right)}{\cos\alpha_c} \end{array}\right\}$$

The relation between modulation index (m_01) and the crossover angle (α_c) in overmodulation region 1 is shown in Fig.2-11 (firm line). Since, α_c cannot be explicitly expressed in terms of m_01 ; hence, a predefined look-up table describing the $\alpha_c - m$ relation has been a normal practice to read α_c from m. This leads to the pulse width resolution problem associated with large consumption of processor memory. Here,

the crossover angle (α_c) is estimated directly from the modulation factor (m_01) using Newton's forward interpolation (NFI) **[**33**].**

According to NFI (Appendix A), in the overmodulation region 1, the crossover angle (α_C) as a function of modulation index (m) is given by (2-33) as:

$$\alpha_C = \alpha_{c1} + (m\_01 - m_{o11})k_1 + (m\_01 - m_{o11})(m\_01 - m_{o12})k_2 + \cdots + (m\_01 - m_{o11})(m\_01 - m_{o12}) \cdot (m\_01 - m_{o110})k_{10}$$

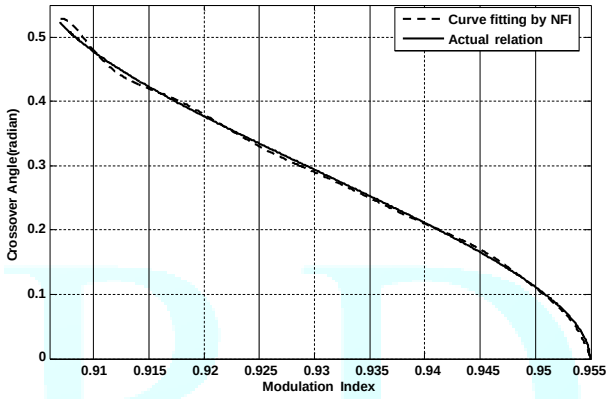

Fig. Modulation index relation with crossover angle in overmodulation region 1 by NFI and Actual analysis

For the present case 8 pairs of discrete values of (m_01, α_c) are chosen from the exact curve of Fig.2-11 (firm line) to form the function (2-44). The m_{o1i} and k_i values (for $i = 1,2,.....,8$) used in (2-44) are given in Table 2.2.The region 1 ends when $\alpha_{c1} = 0$ at $m\_01 = 0.955$.

The dotted line in Fig. shows the $\alpha_C - m$ relation obtained by NFI. It can be concluded that as the curve-fitting by NFI is very much satisfactory.

Table 2.2 m_{bj} and k_i values for estimating the functions in overmodulation region 1 ($j=1$) and region 2 ($j=2$)

m_{bj}	m_{oj1}	m_{oj2}	m_{oj3}	m_{oj4}	m_{oj5}	m_{oj6}	m_{oj7}	m_{oj8}
Mode-I	0.955	0.950	0.945	0.940	0.935	0.930	0.925	0.920
Mode-II	0.955	0.960	0.965	0.970	0.975	0.980	0.985	0.990
k_i	$k_1 = \frac{\Delta y_1}{h}$	$k_2 = \frac{\Delta^2 y_1}{h^2 \times 2!}$	$k_3 = \frac{\Delta^3 y_1}{h^3 \times 3!}$	$k_4 = \frac{\Delta^4 y_1}{h^4 \times 4!}$	$k_5 = \frac{\Delta^5 y_1}{h^5 \times 5!}$	$k_6 = \frac{\Delta^6 y_1}{h^6 \times 6!}$	$k_7 = \frac{\Delta^7 y_1}{h^7 \times 7!}$	$k_8 = \frac{\Delta^8 y_1}{h^8 \times 8!}$
Mode-I	–22.0	–1000.0	-4×10^4	-6.66×10^5	2.66×10^7	2.66×10^9	1.01×10^{11}	0.144
Mode-II	6.0	6.94×10^{-14}	1.33×10^4	-1.33×10^6	8.00×10^7	-3.55×10^9	1.52×10^{11}	-5.71×10^{12}

1.2 Overmodulation region-2

At the end of region 1, the component of the reference voltage changes to a piecewise linear waveform tending towards square-wave mode operation. When the modulation index is higher than 0.952, the second region of overmodulation is entered. The actual trajectory has to be modified so that the reference voltage matches the output fundamental voltage. As depicted in Fig.2-12 holding angle α_h holds the modified reference vector at the vertex of hexagon and for rest of the switching period it track the hexagon side in every sector. The magnitude of V_{an} remains constant during holding period whereas, changes linearly during the hexagon trajectory. Fig.2-13 shows the trajectory of the reference voltage vector and phase voltage waveform in the overmodulation region 2 and the voltage equations in four segments are expressed as follows

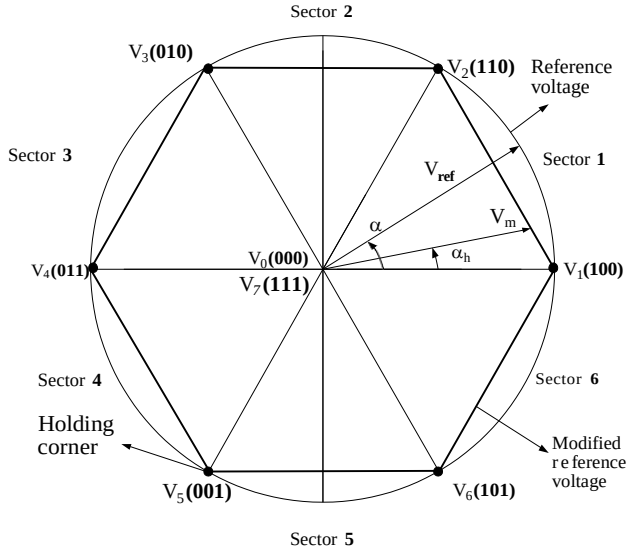

Fig. Space vectors of three-phase inverter showing reference voltage trajectory and segments of adjacent voltage vectors for overmodulation region 2

$$f_1 = m_1,\theta \qquad 0 \le \theta \le \left(\frac{\pi}{6} - \alpha_h\right)$$

$$f_2 = \frac{V_{dc}}{3}, \qquad \left(\frac{\pi}{6} - \alpha_h\right) \le \theta \le \left(\frac{\pi}{6} + \alpha_h\right)$$

$$f_3 = A + m_2\,\theta, \qquad \left(\frac{\pi}{6} + \alpha_h\right) \le \theta \le \left(\frac{\pi}{2} - \alpha_h\right)$$

$$f_4 = \frac{2}{3}V_{dc} \qquad \left(\frac{\pi}{2} - \alpha_h\right) \le \theta \le \frac{\pi}{2}$$

$$\text{Where, } m_1 = \frac{V_{dc}}{3\left(\frac{\pi}{6} - \alpha_h\right)};\ m_2 = \frac{V_{dc}}{3\left(\frac{\pi}{3} - 2\alpha_h\right)};\ A = \frac{V_{dc}3\left(\frac{\pi}{6} - 3\alpha_h\right)}{3\left(\frac{\pi}{3} - 2\alpha_h\right)}$$

Hence, the peak value of the fundamental output voltage (V_{1_mod2}) can be found with the help of Fourier series expansion

$$V_{1\_mod2} = \frac{4}{\pi}\left[\int_{0}^{\pi/6-\alpha_h} f_1 \sin\theta\, d\theta + \int_{\pi/6-\alpha_h}^{\pi/6+\alpha_h} f_2 \sin\theta\, d\theta + \int_{\pi/6+\alpha_h}^{\pi/2-\alpha_h} f_3 \sin\theta\, d\theta + \int_{\pi/2-\alpha_h}^{\pi/2} f_4 \sin\theta\, d\theta\right]$$

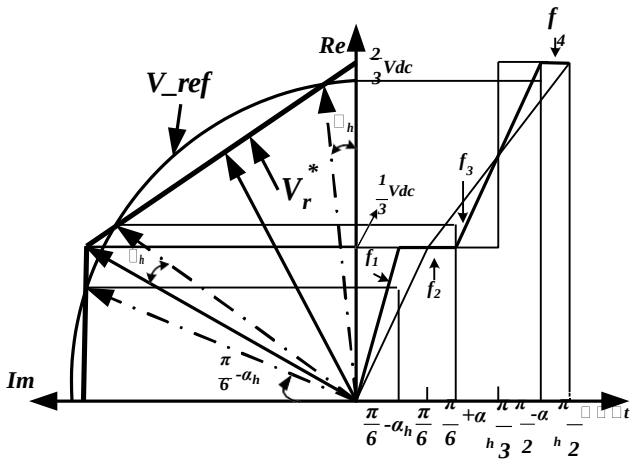

Fig. Trajectory of reference voltage vector and phase voltage for waveform for overmodulation region 2

Therefore, using the modulation factor in the overmodulation region 2 is given as:

$$m\_o2 = \frac{\sin\left(\frac{\pi}{6} - \alpha_h\right)}{\left(\frac{\pi}{6} - \alpha_h\right)} \qquad (2\text{-}50)$$

The relation between modulation index (m_o2) and the holding angle (α_h) in overmodulation region 2 is shown in Fig.2-14 (firm line). It is obvious form (2-50) that (α_h) cannot be explicitly expressed in terms of m_o2 ; hence, alike region 1, the holding angle (α_h) is estimated directly from the modulation factor (m_o2) using Newton's forward interpolation (NFI).

Therefore, according to NFI, in the overmodulation region-2, the holding angle (α_h) function of modulation factor (m_o2) is given as:

$$\alpha_h = \alpha_{h1} + (m\_o2 - m_{o21})k_1 + (m\_o2 - m_{o21})(m\_o2 - m_{o22})k_2 + \cdots + (m\_o2 - m_{o21})(m\_o2 - m_{o22})\cdots(m\_o2 - m_{o29})k_9$$

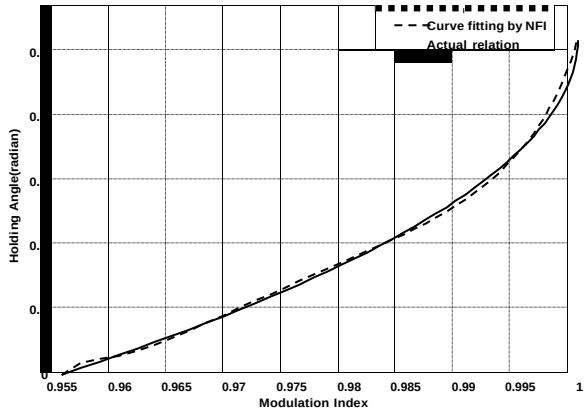

Fig. Modulation index relation with holding angle in overmodulation region 2 by NFI and Actual analysis

In this occasion 8 pairs of discrete values of (m_o2,α_h) are chosen from the exact curve of Fig.2-14 (firm line) to form the function (2-51). The m_{o2i} and k_i values (for $i=1,2,\cdots.8$) used in are given in Table 2.2. The region 2 ends when $\alpha_h=\pi/6$ at $m\_o2=1$. At this condition linear segments vanish, resulting a square-wave operation. In (2-51), α_{h1} is considered as zero at the start of region 2 where $m\_o2=0.955$ (Fig.2-14).

The dotted line in Fig.2-13 shows the m_o2-α_h relation obtained by NFI. In this region also a satisfactory curve-fitting is obtained.

2. SIMULATION:

➢ *Calculation of crossover angle α_c ,holding angle α_h and modified reference voltage:*

The magnitude of reference voltage decides the modulation region. If $(|V_{ref}|)$ lies in the range of $(0\ to\ 0.577)V_{dc}$ then SVPWM works in undermodulation region. During this range modified reference voltage is equal to reference voltage and angle remains the same as calculated in (4-7). Overmodulation region 1 lies between $(0.577\ to\ 0.6061)V_{dc}$.In this range crossover angle is used instead of angle which is calculated by using Newton's forward interpolation as discussed in chapter 2 (2-44). Modified reference voltage is calculated by using.(2-41) When $(|V_{ref}|)$ lies in range $(0.6061\ to\ 0.6366)V_{dc}$ SVPWM works in Overmodulation region 2 during this region holding angle α_h is also calculated by Newton's forward interpolation.

➢ *Calculation of turn-on time of phases*

After calculating crossover angle α_c ,holding angle α_h and modified reference voltage turn-on time of each phase is calculated by using following expression.

Phase A turn-on time for undermodulation region is as follows

$$T_A = T_s/4 + (V_m) \times g(\theta)$$

$$\text{Where, } g(\theta) = \begin{cases} K[-\sin(\pi/3 - \theta) - \sin(\theta)], & S = 1,6 \\ K[-\sin(\pi/3 - \theta) + \sin(\theta)], & S = 2 \\ K[\sin(\pi/3 - \theta) + \sin(\theta)], & S = 3,4 \\ K[\sin(\pi/3 - \theta) - \sin(\theta)], & S = 5 \end{cases}$$

$V_m = V_{ref}$

$K = (\sqrt{3}T_s)/(4V_{dc})$ and S represents different sectors.

The turn-on time for phases B, C are similar to turn-on T_A with phase shift of -120^0 and $+120^0$ respectively obtained for different sectors using (4-8). Turn-on time for phase A as a function of time is shown in Fig.4.6.

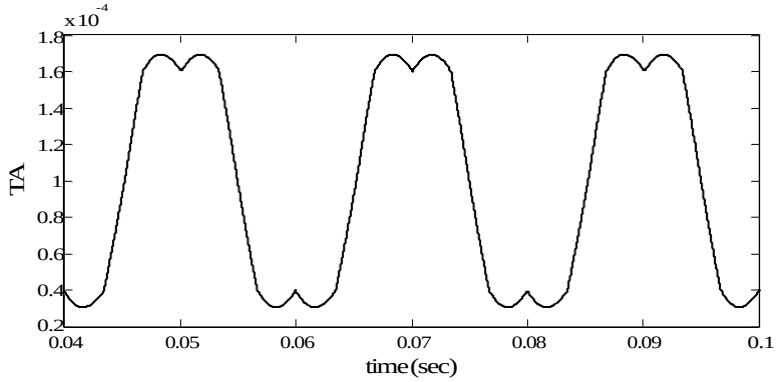

Fig. 4-6 Turn-on time as a function of time for modulation index=0.9063(undermodulation region)

Phase A turn-on time for Overmodulation region 1 is as follows

As already mentioned, Overmodulation region-1 is characterized by a part of hexagon and a part of circle. As circle trajectory is linear in nature, turn-on time in this region is same as undermodulation region

During hexagon trajectory zero vectors vanishes and T_A is expressed as and shown in Fig. as function of time.

$$T_A = \begin{cases} 0, & S = 1,6 \\ \frac{T_s}{2} - \frac{T_s}{2}\left[\frac{\sqrt{3}\cos\alpha_t - \sin\alpha_t}{\sqrt{3}\cos\alpha_t + \sin\alpha_t}\right], & S = 2 \\ \frac{T_s}{2}, & S = 3,4 \\ \frac{T_s}{2}\left[\frac{\sqrt{3}\cos\alpha_t - \sin\alpha_t}{\sqrt{3}\cos\alpha_t + \sin\alpha_t}\right], & S = 5 \end{cases}$$

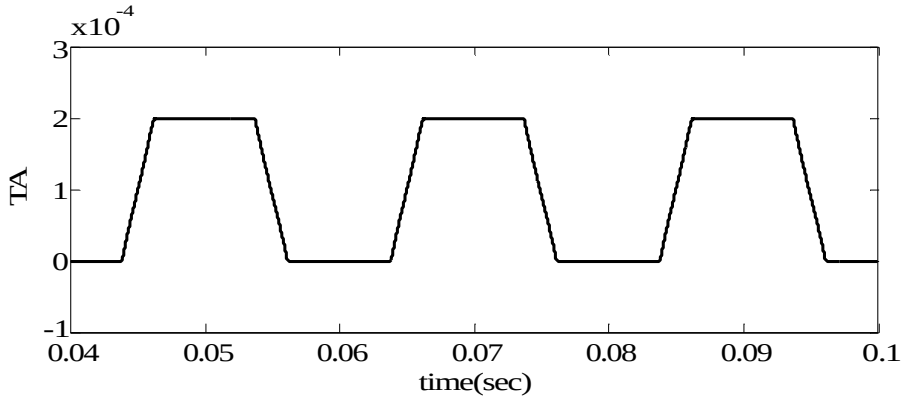

Fig. 4-7 Turn-on time as a function of time for modulation index=0.9425(overmodulation region 1)

Phase A turn-on time for Overmodulation region 2 is as follows

In this region modified reference voltage is partly hold at vertex of hexagon by holding angle α_h .Thus T_A for this part is same as that of Overmodulation region 1 for hexagonal trajectory, except replacing α_c by α_h .

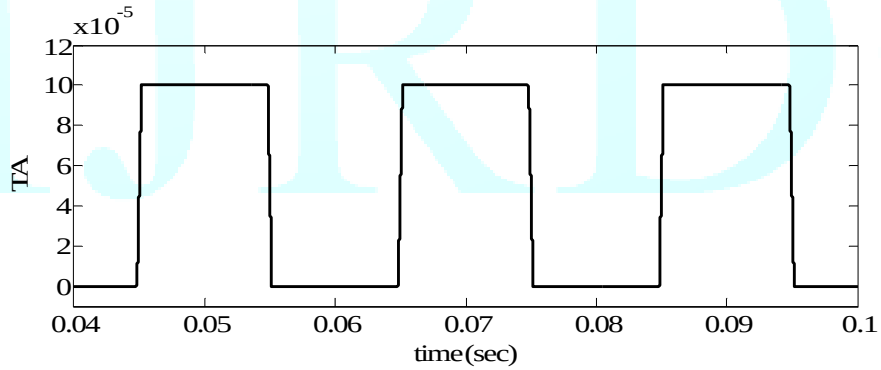

Fig. Turn-on time as a function of time for modulation index=0.9927 (overmodulation region 2)

- *Pulse generation*

Pulses for inverter switches are generated by comparing T_A, T_B, T_C with high frequency triangle carrier wave by using comparator separately for each phase. The output of each comparator is applied at its respective leg of inverter.

The pole voltages V_{A0}, V_{B0}, V_{C0} obtained as output of inverter are converted to line-to-neutral voltages by using following expressions and waveforms are depicted in Fig.

$$V_{AN} = \frac{2}{3}V_{A0} - \frac{1}{3}V_{B0} - \frac{1}{3}V_{C0}$$

$$V_{BN} = \frac{2}{3}V_{B0} - \frac{1}{3}V_{A0} - \frac{1}{3}V_{C0}$$

$$V_{CN} = \frac{2}{3}V_{C0} - \frac{1}{3}V_{A0} - \frac{1}{3}V_{B0}$$

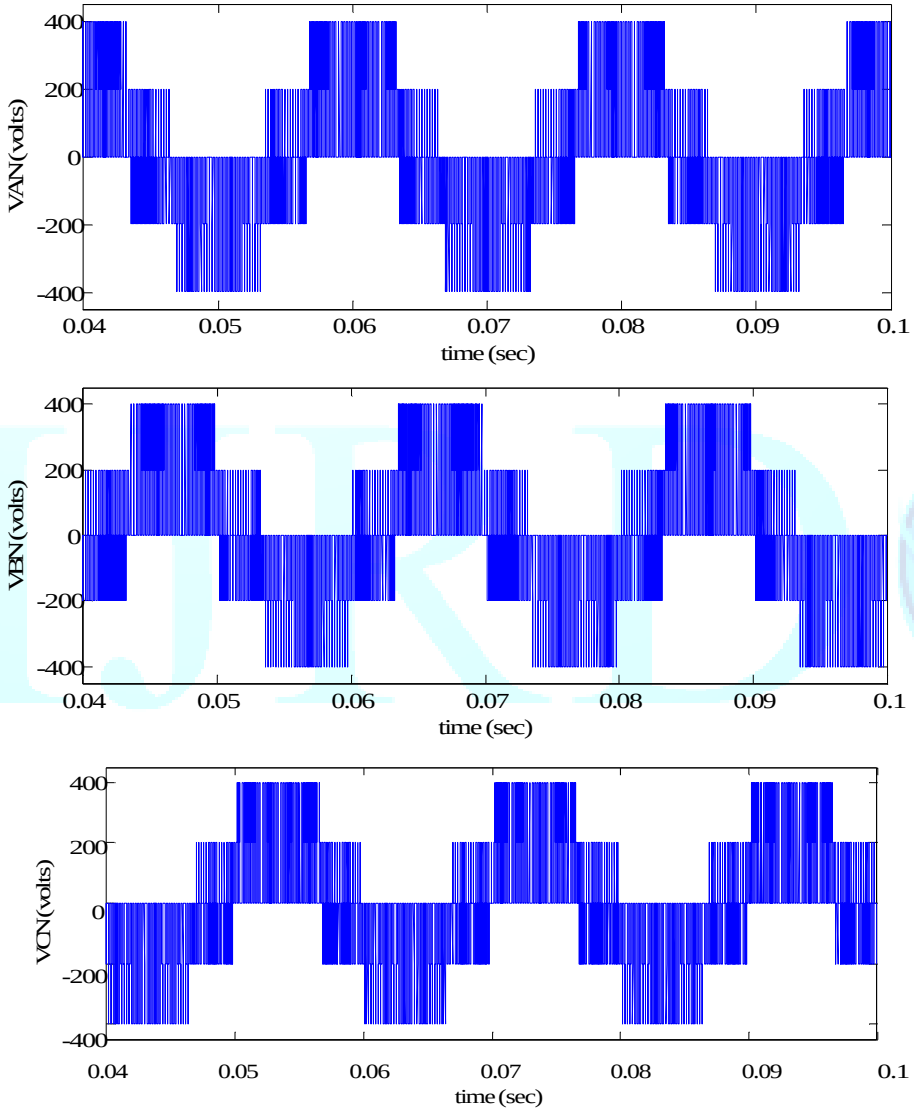

Fig. Line to neutral voltages of three-phase SVPWM inverter

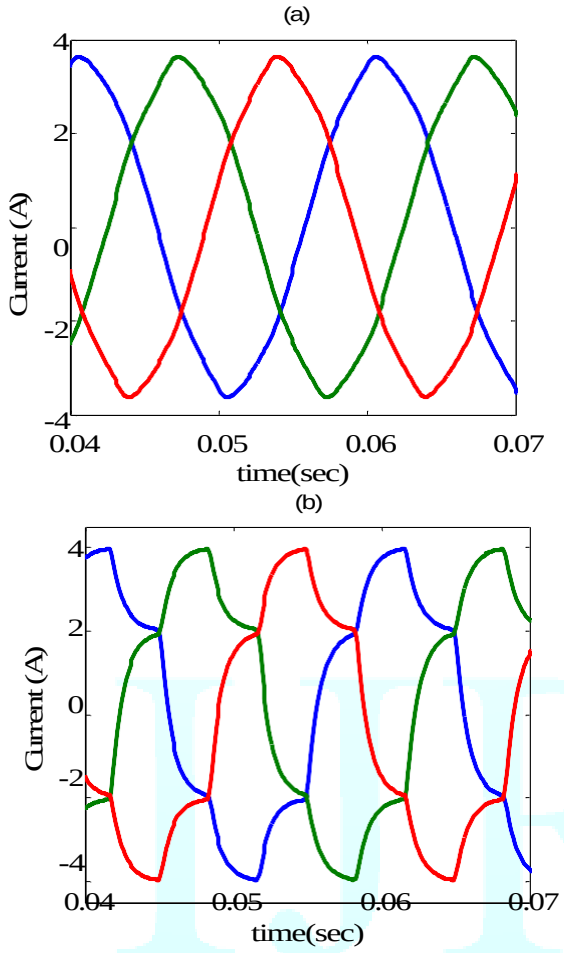

Filtered current waveforms (a)overmodulation region 1 (b) overmodulation region 2

2.1 Results and Discussion

Total Harmonic Distortion: The ratio of the root-mean-square of the harmonic content to the root-mean-square value of the fundamental quantity expressed as a percent of the fundamental.

$$THD = \sqrt{\frac{sum\ \ of\ \ squares\ of\ \ amplitudes\ of\ \ all\ \ harmonics}{square\ of\ \ amplitude\ of\ \ fundamental}}.100\%$$

THD of phase voltage and current is measured using FFT analysis tool for SPWM and SVPWM (undermodulation region) at different switching frequencies and the result is shown in Table

Table Simulation results: THD (%) in phase currents using SVPWM technique

Modulation region	MI	$F_s = 5\ kHz\ T_L = 3.5\ Nm$ THD (%) in phase current	$F_s = 10kHz\ T_L = 1Nm$ THD (%) in phase current	Conventional
Overmodulation-1	0.9267	15.4	6.5	
Overmodulation-2	0.9738	35.9	15.2	

REFERENCES

[1] FangZhengPeng, Jih-ShengLai, and et al, "A multilevel voltage-source inverter with separate dc sources for static sar gneration," *IEEE Trans. on Industry Applications*, vol. 32, no. 5, pp. 1130-1138, September/October 1996.

[2] B.K. Bose, *Modern power electrics and ac drives*.: Prentice-Hall, 2002.

[3] B.K. Bose, "An adaptive hysteresis-band current control technique of a voltage -fed PWM inverter for machine drive sysytem," *IEEE Trans. On Industrial Electronics*, vol. 37, no. 5, pp. 402-408, 1990.

[4] M.Lafor and I.J.Iglesias, "A novel double hysteresis-band current control for a three-level volage source inverter," *3 1st Annual Power Ele"ies Specialist Conference*, vol. 1, p. 21.

[5] J.Y.Lee and Y.Y.Sun, "A new SPWM inverter with minimum filter requirement," *International Journal of Electronics*, vol. 64, no. 5, pp. 815-826, 1988.

[6] Nazmul Islam Raju, Md. Shahinur Islam, and Ahmed Ahsan Uddin, "Sinusoidal PWM signal generation technique for three phase voltage source inverter with analog circuit & simulation of PWM

inverter for standalone load & micro-grid system," *INTERNATIONAL JOURNAL of RENEWABLE ENERGY RESEARCH* , vol. 3, no. 3.

[7] L.Lei, W.Tian-yu, and X. Wen-guo, "Application of sinusoidal pulse width modulation algorithm in the grid-connected photovoltaic system," *Int. Conf. Inf. Technol., Comput. Eng. Manage. Sci.*, vol. 2, pp. 254-257, 2011.

[8] M.Suetake, I.N.da Silva, and A.Goedtel, "Embedded DSP-based compact fuzzy system and its application for induction-motor V/f speed control," *IEEE Trans. Ind. Electron.*, vol. 58, no. 3, pp. 750-760, Mar. 2011.

[9] AHMAD SHUKRI FAZIL RAHMAN et al., "Microcontroller based SPWM generator: A conventional design perspective through gaphical oriented approach," *NTERNATIONAL JOURNAL OF INNOVATIVE TECHNOLOGY AND RESEARCH*, vol. 1, no. 3, pp. 226-232, April-May 2013.

[10] A.Maiti, S.Choudhuri, J. Bera, T. Banerjee, and S.Maitra, "Development of microcontroller based single phase SPWM inverter with remote control facility," *Joint Int. Conf. Power Electron., Drives Energy Syst./Power India*, pp. 1-5, 2010.

[11] M. F. N. Tajuddin, N. H. Ghazali, I. Daut, and B. Ismail, "Implementation of DSP based SPWM for single phase inverter," *Int. Symp. Power Electron. Electr. Drives Autom. Motion*, pp. 1129-1134, 2010.

[12] W. Song, Z. Xiaoli, Y. Dongxuan, L. Xiaoqin, and H. Aihong, "Design of photovoltaic inverter system based on TMS320F28027," *Int. Conf. Comput. Appl. Syst. Model.*, vol. 2, pp. 43-47, 2010.

[13] R.K.Pongiannan and N.Yadaiah, "FPGA based three phase sinusoidal PWM," *International Conference on Electrical Energy*, pp. 34-39, 2011.

[14] M.A.Rongi, A.Saparon, and M. K.Hamzah, "Sinusoidal pulse width modulation using CORDIC algorithm for single phase matrix converter," *IEEE 5th Conf. Ind. Electron.Appl.*, pp. 1088-1093, Jun. 2010.

[15] G.Shuangxi, C.Shufu, and Z.Ying, "Sinusoidal pulse width modulation design based DDS," pp. 1-4.

[16] Z.Chongqing and C.Jianli, "A new method of solving SPWM switch point based on natural sampling," pp. 325-329.

[17] L.Fan, L.Kun, and L. Yang, "A design and implementation of edge controller for SPWM waves ," 764-767.